Materials Research. 2025; 28(suppl. 1): e20250272
DOI: https://doi.org/10.1590/1980-5373-MR-2025-0272

Recycling and Processing of Plastics by Ionizing and Non-Ionizing Radiation: Evaluation of the Polypropylene from Recycled Packaging and Environmental Tests on Plants

***Julio Harada*[a], *Juliana Arquinto*[a*], *Maria da Conceição Costa Pereira*[a],**

***Maria Elizabeth Maués dos Santos*[a], *Dione Pereira de Castro*[a],**

***Leonardo Gondim de Andrade e Silva*[a]**

[a]*Comissão Nacional de Energia Nuclear, Instituto de Pesquisas Energéticas e Nucleares, São Paulo, SP, Brasil.*

Received: January 31, 2025; Revised: July 25, 2025; Accepted: August 03, 2025

Plastic waste contributes negatively to the environment by increasing space occupation, creating health hazards on land, in the air, and at sea. For this reason, they need to be disposed of properly so that they can be recycled efficiently. To combat these impacts and reduce environmental pollution, this project aims to study the recycling process of polypropylene (PP) from industrial waste scraps and polypropylene from urban solid waste (MSW) using ionizing radiation from 0 to 500 kGy. Irradiation processing showed efficiency when compared to other recycling processes, promoting the molecular shearing of PP, reaching ideal lengths of shorter chains to be used as a carrier for additives for adhesives and plastics, and/or to be used as a flow modifier for injecting parts. Ionizing radiation above 100 kGy initiated the formation of cross-links, cross-linking the PP that could be used as fillers for asphalt, construction, and other applications, or as a fuel energy source, contributing to the ecosystem, without changes in the curly lettuce after ecotoxicity tests. The use of ionizing radiation in polymer processing has a great advantage when compared to other plastic recycling systems.

Keywords: *Recycling, recyclable plastics, ionizing radiation, polypropylene, environmental tests.*

1. Introduction

The growth of consumption led to an intense process of environmental degradation through the production of high levels of waste and high energy consumption, threatening natural and energy resources[1]. The use of waste is of fundamental importance as it avoids improper disposal and minimizes the consumption of natural resources[1-3]. In this way, the use of non-biodegradable waste to produce fuels, naphtha (raw material for polymers), and energy is a promising alternative because, in the event of major discoveries and improvements in conversion technologies, two of today's major problems could be solved[2].

The combustion of plastic parts and packaging produces toxic gases that can contain carcinogenic and mutagenic chemicals[4], just as the incineration of plastic parts and packaging requires expensive systems to control polluting gas emissions. In landfills, plastic parts and packaging are not easily degraded due to their shape and impermeability; they store water for a long period, enabling breeding sites for mosquito larvae that are vectors of diseases such as dengue, chikungunya, zika, and malaria[5]. Polypropylene (PP) is the fastest-growing commodity resin due to its advantageous physical properties, including low weight, recyclability, and chemical resistance. As the lightest known industrial material, it is widely used across various industries[6].

Rigid and flexible plastic components and packaging are among the most prevalent waste products generated by urban expansion, where the population grows exponentially, the production of these plastic materials also increases, with the technology ever advancing[3], especially the polypropylene with a higher modulus of strength and lower impact strength and strains at yielding and failure[3,6,7]. Although the blending of virgin and recycled polypropylene has been extensively studied, most research utilizes commercially sourced recycled PP (PPrec) with unknown or inconsistent composition, often containing contaminants like other polymers[8].

Therefore, when post-consumer PPrec with an extensive weathering history undergoes melt processing, chain scission leads to a reduction in its molecular weight[1,8,9]. As plastic parts and packaging are mainly made up of long-chain hydrocarbons, reprocessing them could provide an economical way of treating these discarded plastic parts and packaging (waste)[8], recovering them as a source of valuable hydrocarbons and also for the supply of other chemical products[2,10]. Compared to coal, plastic parts and packaging have a higher calorific value, as well as a considerable number of fillers used in their composition[3]. It is therefore understandable to develop technologies to harness their high energy potential to continue the search for alternative

*e-mail: juliana_arquinto@hotmail.com
Associate Editor: Walney Araújo.
Editor-in-Chief: Luiz Antonio Pessan.

fuels, reduce and mitigate CO_2 emissions, and reduce and/or recycle raw materials[7].

In this context, irradiation is gaining significant attention as a technology for recovering energy from plastic waste. Unlike combustion or incineration, irradiation operates in an oxygen-free (inert) atmosphere, preventing the formation of highly toxic and polluting oxygenated compounds such as dioxins and furans[4].

Irradiation is a promising technological alternative for treating plastic waste, as it produces three fractions with different potential applications[1,10,11]. Ionizing radiation interacts with polymers, causing ionization and excitation of the polymer molecules, which results in the material becoming chemically unstable[12]. These macroradicals are prone to the β-chain-scission reaction, and therefore the average molar mass (Mw) of polypropylene (PP) is decreased[1,12]. Zerhusen et al.[9] evaluate the influence of γ-radiation sterilization (48–52 kGy) on the repetitive injection molding of a polypropylene copolymer, whereas the non-showing influence of repetitive processing did not show any measurable differences after the irradiation process. The e-beam method enhances the melt strength of PP by generating macroradicals, and a comparable correlation between PE impurity levels and gel content is anticipated. This study focuses on assessing this radiation-applied effect[1,9,11]. The specimens were irradiated at different doses, followed by the determination of the chemical and physical properties. Additionally, the PP irradiated was subjected to injection molding trays to assess technical processability and to determine chemical and mechanical properties. Finally, environmental test measurements were used to estimate the influence of the PPrec on plants.

2. Materials and Methods

The recycled polypropylene pellets (PPrec) used in this work came from CLEAN ECO® (Batch 0182350099), for agricultural trays injected and supplied by the JKS® company. Figure 1 shows a sample of the CLEAN ECO® (PPrec) used in the injection of agricultural trays and for planting seedlings. The samples of PPrec are suitable for injection molding and were obtained from industrial waste and selective waste collection (MSW).

2.1. Injection sample

The selected granulated material was injected into the Battenfeld® injection molding machine, following parameters as indicated by the resin supplier: temperature profile of 250/250/260/270°C from the feed to the nozzle, with injection pressure around 160 bar, mold temperature of 60°C, injection speed of 22 mm/min, cooling time of 20 s, total cycle of 35 s. Figure 2 shows some of the specimens injected for characterization.

2.2. Irradiation samples

The samples of PPrec, the test specimens, and the trays were exposed to ionizing radiation for further characterization. The irradiation treatment was performed in the Dynamitron® Job 188 electron accelerator (Radiation Dynamics, Inc.) available at the IPEN-CNEN. The samples were irradiated with the doses as follows: 0, 12.5, 25, 150, 200, 250, 300, 350, 430, 500 kGy. The injected agricultural trays were also subjected to different low doses of radiation to assess possible toxicological effects.

2.3. Polypropylene recycled characterization (PPrec)

The X-ray diffraction (XRD) patterns were obtained using a Rigaku Multiflex™ diffractometer (Rigaku®, Tokyo, Japan) set to operate at 40 kV, with Cu-Kα radiation (λ = 1.541 Å). The XRD measurements were conducted over a 2θ range up to 60°, with a step increment of 0.06° and a scanning rate of 4 s. The crystallinity index (CI%) measured for the samples was calculated from XRD spectra, using the Rietveld refinement[13,14] with the support of the Bruker DIFFRAC. EVA™ software. The ratio between crystalline and amorphous areas was measured according to Equation 1:

$$CI\ \% = \left(\frac{C_a}{T_a}\right) * 100 \quad (1)$$

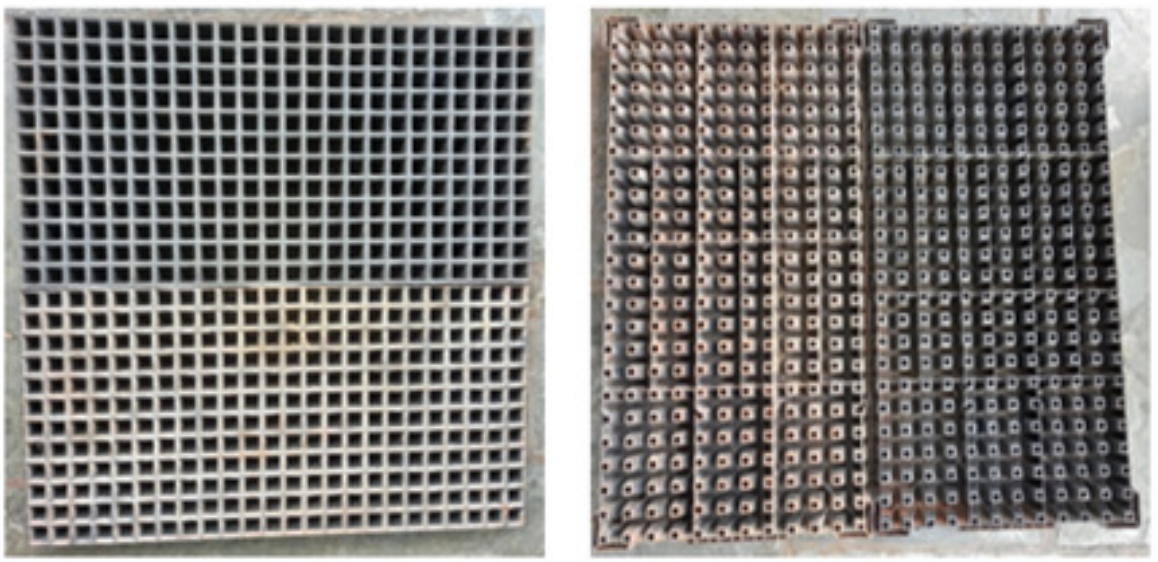

Figure 1. Agricultural trays made of PPrec grafted trays. Front (left) and back (right).

Figure 2. Injected PP specimens.

Where CI% = crystallinity index; Ca is the crystallinity area, and Ta is the total area.

The Fourier transform infrared spectroscopy (FTIR) spectra measurements were performed at the 450–4000 cm^{-1} range, using 32 scans and a 4 cm^{-1} resolution, in a PerkinElmer Spectrum 3™ (PerkinElmer®, United Kingdom) spectrometer. The samples were analyzed in a UATR accessory. The Raman spectroscopy study was carried out using a Raman Horiba® confocal microscope, model XploRA™ PLUS (HORIBA France SAS), provided with a multi-laser with 785 nm in the spectral range of 400 to 2000 Raman shift cm^{-1}. These measurements for FTIR and Raman spectra were performed directly on the surface of the samples, without any previous treatments.

In the scanning electron microscope (SEM) analyses, the samples were analyzed using the JEOL® JSM 6510 Series equipment (JEOL Ltd., Tokyo, Japan), coupled with an EDS (energy dispersive X-ray spectroscopy) device and equipped with a tungsten filament. The samples were first glass-fractured with N_2 and then coated with gold nanoparticles. Micrographs were taken using a voltage of 30 kV at different magnifications, using a report creation software (SMile View™).

The injected PPrec samples (Figure 2) were submitted for tensile strength and elongation (ASTM D638[15]) and impact resistance (ASTM D256[16]), respectively, using an Instron® 5567 equipment. For Izod (ASTM D256[16]) and Charpy (ASTM D6110[17]) tests, Instron® CEAST 9050 impact pendulum equipment, was used. For the surface hardness analysis was carried out according to the ASTM D785[18] standard was used.

The development of the germination and growth of lettuce was analyzed in the different irradiation treatments of the trays and under the same management conditions in terms of nutrition, external exposure, pesticides, and irrigation. The 200-cell JKS Eco® trays were used to sow the Loreane Feltrin™ Curly Lettuce seeds in 9 trays with coconut fiber substrate in May/June 2023 (32 days), and divided into 3 groups (0, 12.5, and 25 kGy). Lettuce plants were placed in a standard greenhouse, and the phytosanitary and fertilization treatments were not performed for the ecotoxicity tests.

Particle size analysis was carried out with a vibratory screening machine to separate the different sizes of PPrec ground, according to ASTM D1921[19] and NBR 7181[20] standards. The particle size method is used to improve and evaluate the surface area of the PPrec and facilitate production of the masterbatches incorporated with PP neat.

Gas chromatography instruments (GC-MS) for PPrec molecular weight (MW) measurements were performed on a 1310 GC device equipped with a TriPlus RSH autosampler and coupled to a Q Exactive mass spectrometer (Thermo Fisher Scientific, USA). Separation of PPrec-MW solvated in trichlorobenzene (TCB) occurred on an Optima 5HT column (12.5 m × 0.25 mm, 0.10 µm; Macherey Nagel, Germany), with helium as reagent gas (flow rate of 1.2 mL/min).

2.4. Statistical analysis

The obtained results of lettuce properties were submitted to a simple analysis of variance (ANOVA). Whenever the null hypothesis was rejected, the means were compared using the Tukey test at a significance level of 5% ($p < 0.05$).

3. Results and Discussion

3.1. Morphological analysis

3.1.1. XRD

Figure 3 shows the XRD curves carried out on PPrec irradiated and non-irradiated samples (0, 12.5, 25, 150, 200, 300, 350, 430, and 500 kGy). To quantify the amorphous phase, XRD analyses were carried out on the PPrec samples, non-irradiated and irradiated with doses of 12.5 and 25.0 kGy. When the PPrec samples irradiated at different dosages were compared, it was found that the features of the three peaks changed (when 2θ was 14°, 16°, 18°, 21°, and 23°), some results were described in the literature[7,12,21,22].

In the XRD patterns, the peaks in which the increase in intensity (%) occurred were identified. The positions of the peaks indicate the planes, and the intensities indicate the position of the atoms in that plane, and the widths of the peaks are related to the degree of crystallinity of the material[7,21,22]. Taking the values of the integrals of the region where the peak appears, concerning the entire diffraction pattern, gives the crystalline fraction in percentages. For the analyses of PPrec, non-irradiated and irradiated with doses of 12.5 and 25 kGy, the results were 6.15, 5.44, and 5.43%, respectively, of the crystalline fraction, leading to the conclusion that radiation decreased the crystallinity of the materials analyzed. The reduction in crystallinity results from degradation processes that diminish the crystallite size

of the materials, ultimately expanding the amorphous region in the PPrec samples irradiated[12].

XRD analysis will be carried out to evaluate and compare the non-irradiated and irradiated PPrec samples at doses of 150, 200, and 250 kGy, as shown in Figure 3.

There was a breakdown of the crystalline cells at 11º, as well as an amorphous region, increasing from 5 to 30º. The semi-crystalline PP is characterized by 2θ peaks at 14.2°, 17.1°, and 18.6° corresponding to α (110), α (040), and α (130) reflections[23]. The samples studied did not show significant interference in the peaks after the high-energy irradiation from 250 kGy up to a 500 kGy dose, and did not change the crystallographic properties after irradiation.

3.1.2. Raman spectroscopy

Figure 4 shows the Raman spectrum curve of the iPP specimen reference, and according to studies carried out by Nielsen et al.[24] to compare the Raman spectrum values of PP neat in the partially crystalline solid state and non-irradiated PPrec samples and those samples irradiated (Figure 5).

It is estimated, the band at 808 cm^{-1} and bands at 974 and 840 cm^{-1} assigned to the C–C stretching mode and the CH_3 rocking mode, respectively, are characteristic of PP, due to the bands being characteristic of crystallization and tacticity of polymer[22,25-27]. Detailed literature reviews on the assignment of the Raman spectra-active lines of isotactic PP can be found[22,27,28]. Where observed that the irradiation process shifts the spectra bands, decreasing of crystallinity of the PPrec, with 12.5 and 25 kGy, under the relative intensity of these bands estimated on the Raman spectra (Figure 5). The difference between the values, as evaluated by these two irradiation doses by Raman spectra, can be explained by the presence of the modification or small/defective crystallites, which can contribute to the intensity of the line at 1312 cm^{-1} for 12.5 and 25 kGy irradiated samples, leading to an expansion of the amorphous region in the spectrum. As the dose increases over time, the crystallite

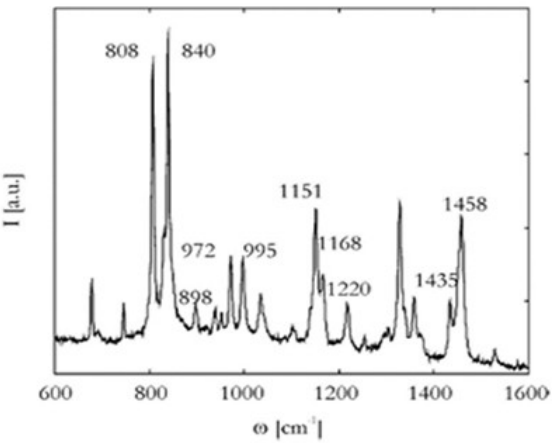

Figure 4. Raman spectra of the iPP specimen, according to the literature[21], for comparison with the Raman shift spectra of PP in the partially crystalline solid state.

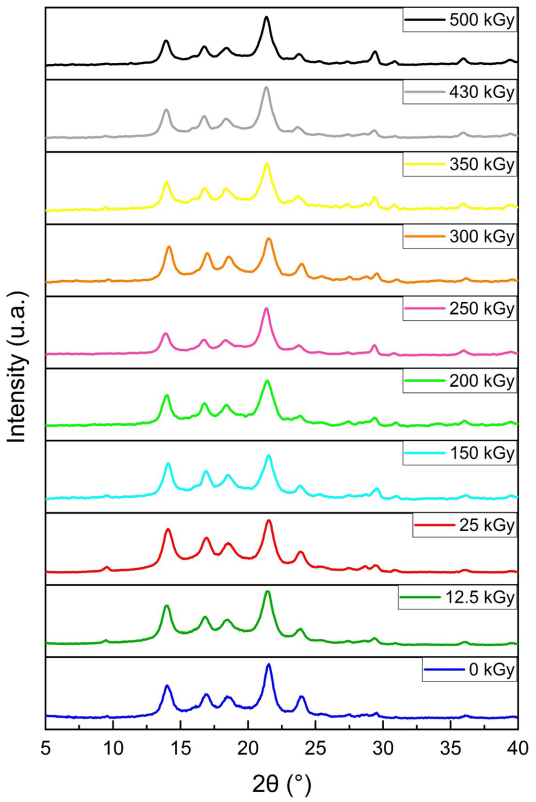

Figure 3. XRD curves of non-irradiated PPrec samples and irradiated with doses of 12.5, 25, 150, 200, 250, 300, 350, 430, and 500 kGy.

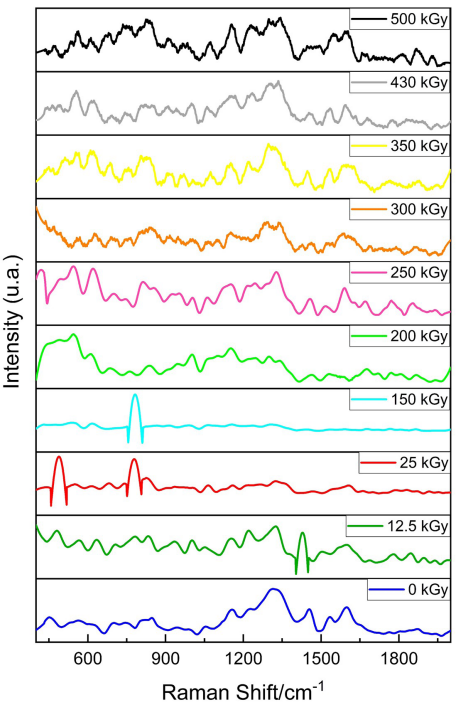

Figure 5. Raman spectra of non-irradiated PPrec samples and irradiated with doses of 12.5, 25, 150, 200, 250, 300, 350, 430, and 500 kGy.

size of the sample decreases due to degradation caused by γ-irradiation, resulting in further growth of the amorphous region and a subsequent reduction in crystallinity[12]. These results are compatible with the other studies[12,22] and analysis XRD performed previously.

Figure 5 shows the Raman spectra of the PPrec samples with doses of 150, 200, and 250 kGy. In the Raman spectrum of PP neat[23], peaks are observed between 500 and 1500 cm^{-1} and from 2600 to 3000 cm^{-1}. Raman spectrum of PP from 500 to 1500 cm^{-1} includes C–C backbone stretching vibrations, $–CH_2–$ deformation, and $–CH_3$ deformation vibrations, and from 2600 to 3000 cm^{-1} includes $–CH_2–$ and $–CH_3$ stretching vibrations. The irradiation doses affected all samples, decreasing their crystallinity with small peaks, and showing more amorphous regions in the PPrec samples irradiated. Pinheiro et al.[28] observed a peak intensity at 1153 cm^{-1}, which shows a slight increase after irradiation, corresponding to the amorphous phase of polypropylene irradiated at 150 kGy dose. Raman peaks at 810 and 842 cm^{-1} regions are due to the vibrations of molecules in the crystalline phase and the vibrations of helical molecules contained in the amorphous regions, respectively.

Figure 6 shows the Raman spectra images of the PPrec samples with doses of 300, 350, 430, and 500 kGy, respectively, for better visualization of the changes that occurred after the irradiation process. Báez et al.[29] and Nielsen et al.[24] stated that, as the intensity of the peak at 810 cm^{-1} increases relative to the intensity of the peak at 842 cm^{-1}, the degree of crystallinity increases in polypropylene, from the observation of correlation splitting. For the samples evaluated, the irradiation doses over 300 kGy do not change the properties of the PPrec samples in this Raman shift range.

3.1.3. FTIR

Figure 7 shows the FTIR curves for the non-irradiated PPrec samples and those irradiated with doses of 150, 200, and 250 kGy. The peaks at 2951 cm^{-1}, 2917 cm^{-1}, and 2848 cm^{-1} are attributed to the asymmetric stretching[23] of the C-H of CH_2. The carboxylic groups of oxidized products[6,30-32] were detected at 1719 cm^{-1}, 1717 cm^{-1}, 1709 cm^{-1}, and the unsaturated groups in the region of 1650 cm^{-1}. The peak at 1457 cm^{-1} is characteristic of the bending and asymmetric deformation of the C-H of CH_3, while the symmetric bending of the CH of the methyl group[23] appears between the peaks at 1376 cm^{-1} and 1365 cm^{-1}. The peaks between 1315 cm^{-1} and 1303 cm^{-1} are due to the CH bending mode, while the peaks at 1167 cm^{-1} and 1019 cm^{-1} represent the C-O-C stretching vibration. The peaks at 973 cm^{-1}, 997 cm^{-1}, and 1165 cm^{-1} are related to the vibration of the CH_3 group, while the peak at 720 cm^{-1} corresponds to the crystalline phase[31,32] of the polymer. Some researchers[32] evaluate that the isotacticity PP peaks (997 cm^{-1} and 973 cm^{-1}) of the polymer may be monitored during the degradation process in soil.

The results found in the FTIR spectroscopy for both the PPrec samples irradiated with low and medium doses of radiation did not alter the composition of the materials present in the PPrec samples, and can be seen in both low and high doses. The decomposition occurs near the surface,

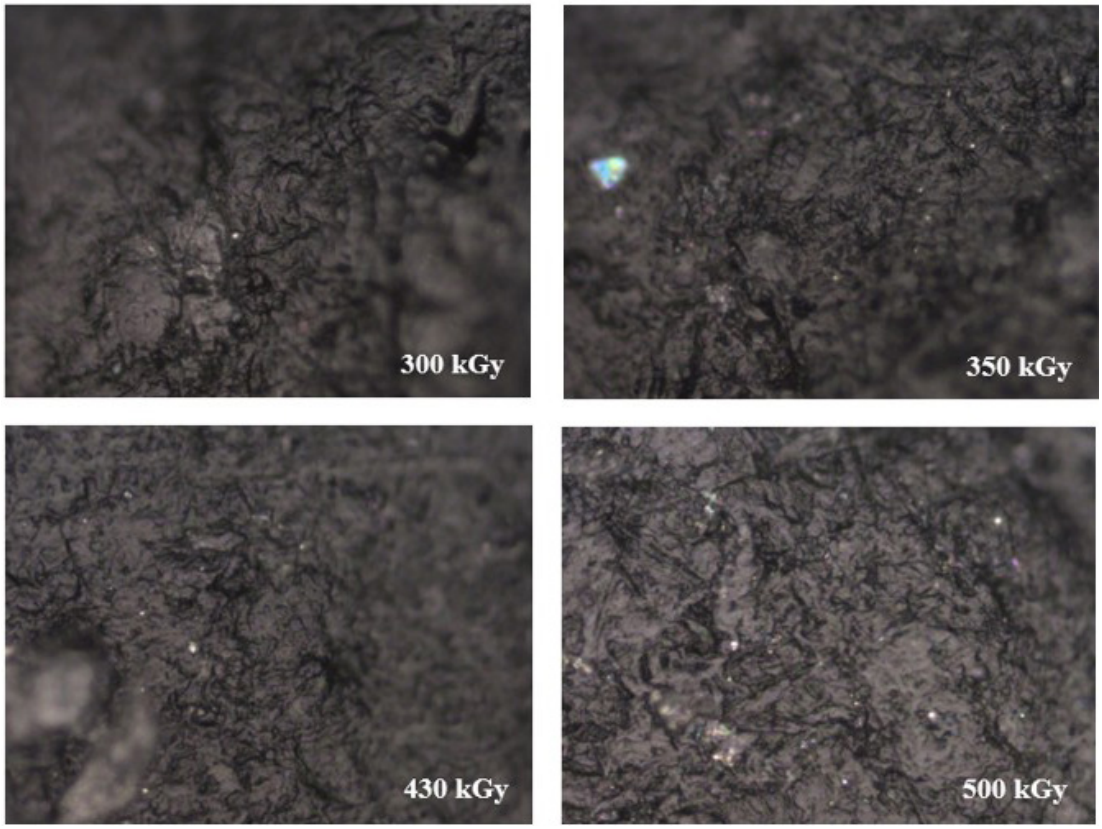

Figure 6. Raman spectroscopy images of PPrec samples irradiated with doses of 300, 350, 430, and 500 kGy.

and the helix length of the PP chain is shortened. H_2, CH_x, and other hydrocarbon fragments, formed by scission of the polypropylene chain[33].

Figure 7 shows the FTIR curves of PPrec samples irradiated with doses of 300, 350, 430, and 500 kGy. Radiolysis in air introduces significant changes in the FTIR spectrum of the PPrec. As a result of irradiation, the intensity and positions of individual absorption bands in the polymer samples change, and new bands appear[31,34]. In the spectra of PPrec irradiated at varying input doses, an absorption band emerges and intensifies within the 3690–3020 cm^{-1} region, displaying characteristic peaks as the irradiation dose increases. The first three bands correspond to the stretching vibrations of -OH groups, with the peak at 3660 cm^{-1} attributed to free -OH groups, while those at 3470 and 3210 cm^{-1} indicate OH groups engaged in intermolecular and intramolecular hydrogen bonding. Additionally, the spectra exhibit a band in the 1820–1660 cm^{-1} region, composed of three overlapping peaks at 1770, 1737, and 1717 cm^{-1}, which correspond to C=O stretching vibrations. A peak at 1610 cm^{-1}, characteristic of C=C stretching in polyenes, is also observed. Further evidence of oxygen-containing groups is provided by peaks at 1240, 1088, and 1053 cm^{-1} in the spectra of irradiated granules. The peak at 1088 cm^{-1} is likely associated with C–O stretching, resulting from reactions with oxygen or water, and may indicate the presence of primary or secondary alcohol groups, though other C–O vibrations could contribute to this broad peak. Finally, peaks at 3080, 728, 610, and 515 cm^{-1} are characteristic of vinyl fragments ($–HC=CH_2$) within the structure of irradiated high doses in the PPrec.

The presence of hydroxyls (-OH) and carbonyl-containing fragments (C=O) in irradiated PPrec results from the radiation-induced oxidation of PP by atmospheric oxygen and moisture[33,34]. Other authors[6,31,35] obtained the specific FTIR spectra from polyolefins, corroborating the results obtained. Some results from this study can be observed and described in the FTIR low and medium-dose data.

3.1.4. SEM

The micrograph of the PP neat specimen (Figure 8) and EDS (Figure 9) correspond to the composition of the elements present in the PP neat pellets.

Figure 10 shows the micrograph of non-irradiated PPrec, at the magnification 700x, 20 µm (a) and 500x, 5 µm (b).

Figure 11 shows the EDS analysis of non-irradiated PPrec and the elements identified.

Figure 12 shows the micrograph of PPrec irradiated at a dose of 12.5 kGy, magnification 700x, 20 µm (a) and 12.5 kGy, magnification 500x, 5 µm (b).

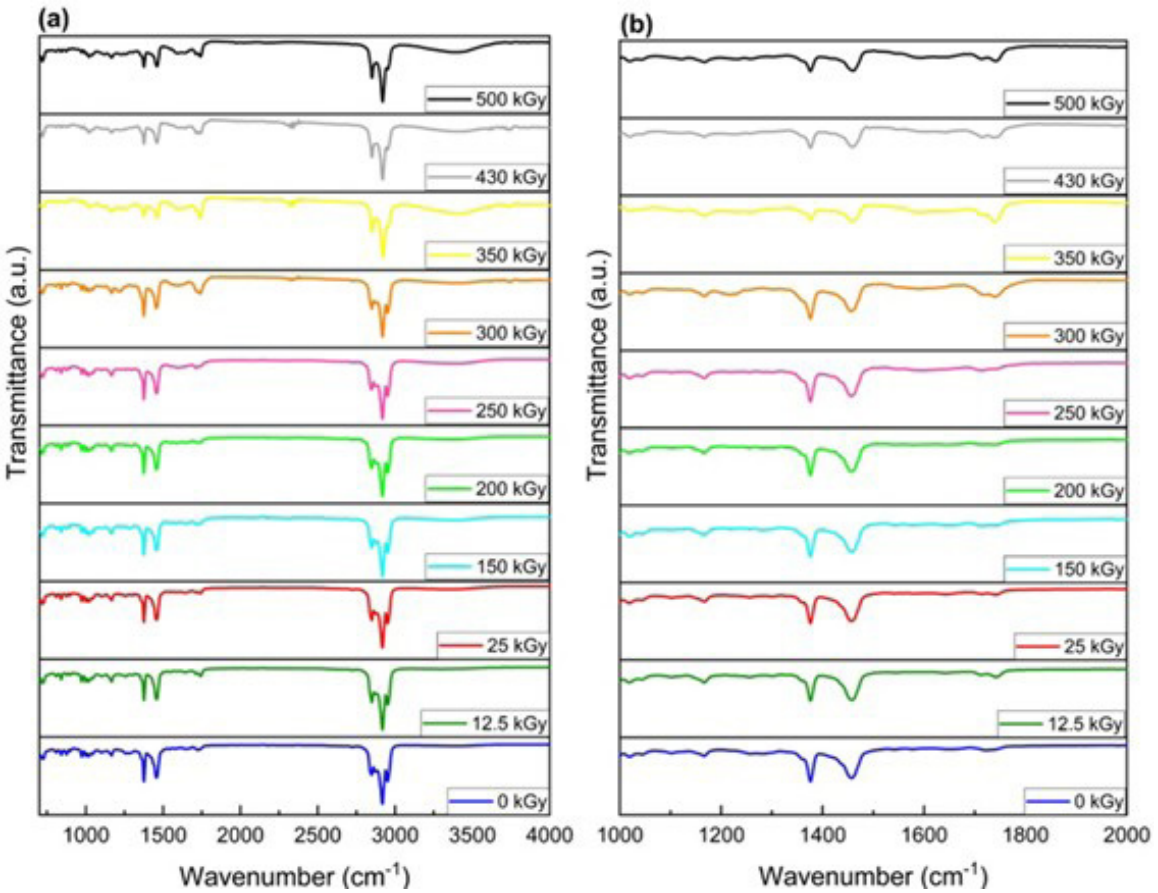

Figure 7. FTIR spectra of non-irradiated PPrec samples and irradiated with doses of 12.5, 25, 150, 200, 250, 300, 350, 430, and 500 kGy. (a) 400-4000 cm^{-1} and zoomed in (b) 1000-2000 cm^{-1}.

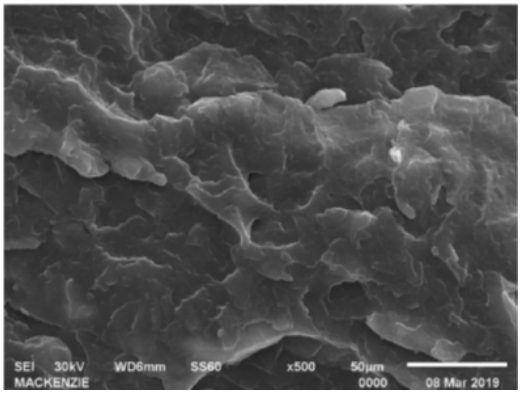

Figure 8. Micrograph of the PP neat specimen, at 500x magnification.

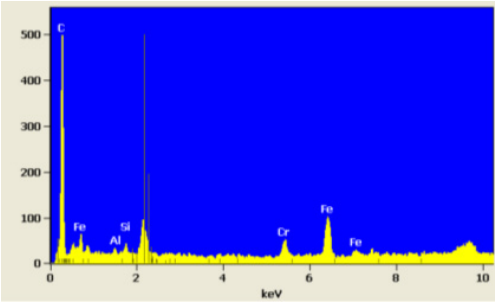

Figure 9. PP neat specimen EDS image.

Figures 13a and 13b shows the micrograph of PPrec irradiated at 25 kGy, magnification 250x, 100 µm, and magnification 500x, 50 µm. There are foreign elements in the PPrec due to the incorporation of inorganic fillers used to improve processing properties and black pigmentation to homogenize the color of the final product, as well as the presence of impurities. These inorganic fillers can be calcium carbonate ($CaCO_3$), zinc stearate (StZn), silica (SiO_2), carbon black, and titanium dioxide (TiO_2). The fracture surface exhibits several features typical: traces of fiber pull-out, dissimilar size of inorganic fillers, and impurities and voids on the specimen were studied[11,21], and the inorganic compounds submitted ($CaCO_3$, StZn, SiO_2, carbon black, and TiO_2), by radiation show an irradiation absorption, avoiding the extended damages in material surface, showed in the EDS images[2].

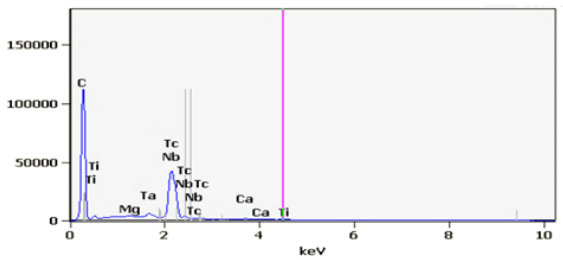

Figure 11. EDS of non-irradiated PPrec specimen.

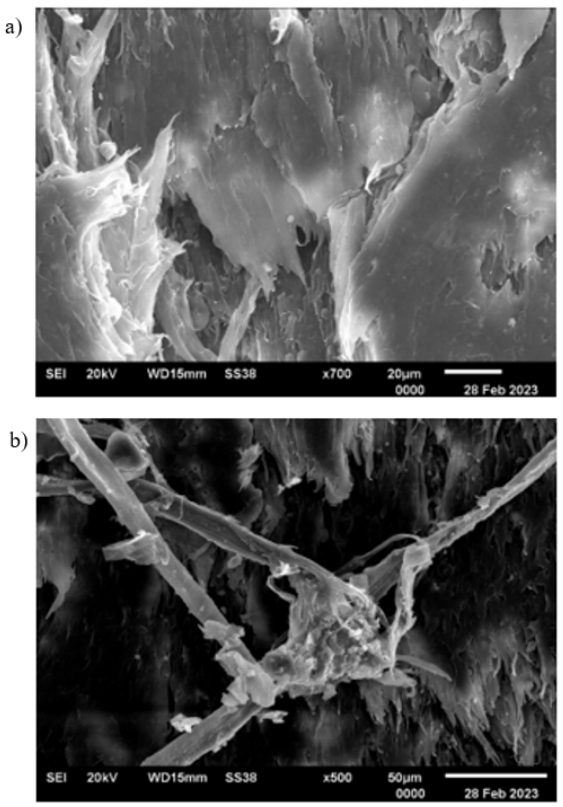

Figure 10. Micrograph of non-irradiated PPrec specimen, magnification 700x, 20 µm (a); 500x, 5 µm (b).

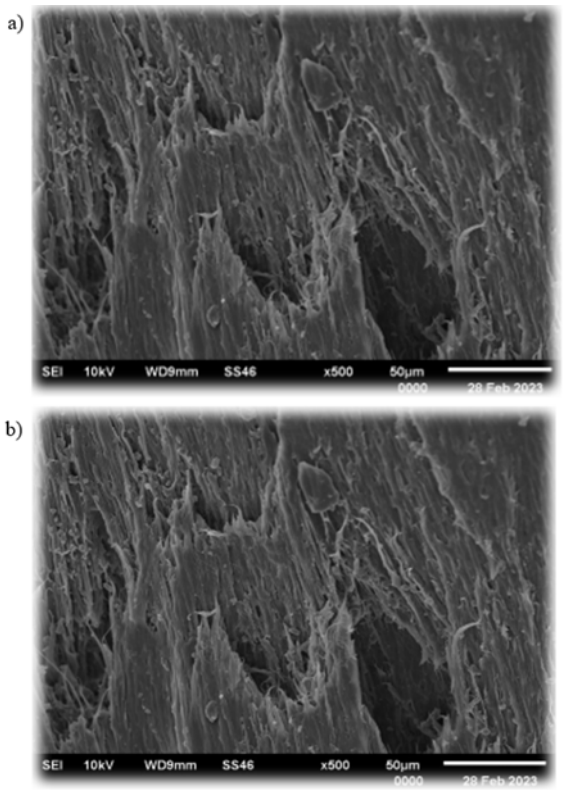

Figure 12. Micrograph of irradiated PPrec specimen, magnification 700x, 20 µm (a); 500x, 5 µm (b).

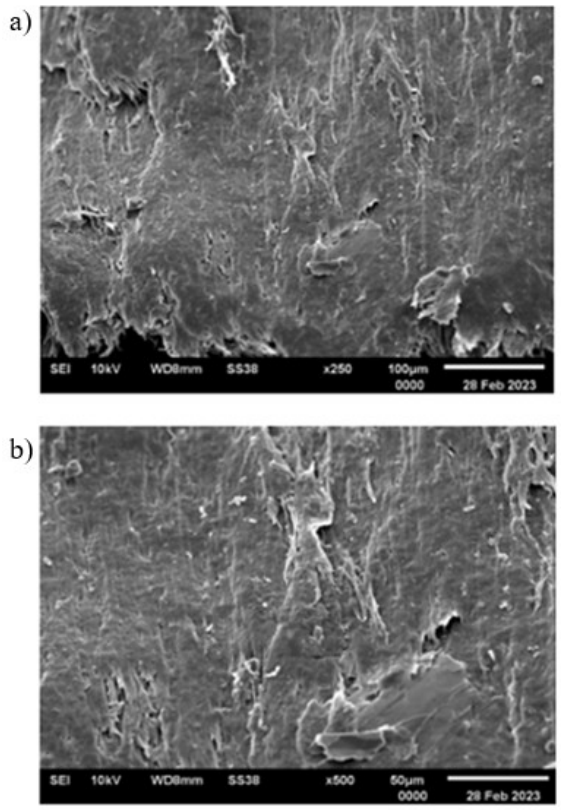

Figure 13. (a) Micrograph of PPrec sample irradiated with dose of 25 kGy, magnification 250x, 100 µm; (b) Micrograph of PPrec sample irradiated with dose of 25 kGy, magnification 500x, 50 µm.

Figures 14a-d shows the SEM micrograph of PPrec with the identification of the elements in different colors and an EDS image sample, irradiated with 12.5 kGy, 400x magnification. Figure 14b shows the EDS with the elements identified, and Figure 14c shows the PPrec micrograph irradiated with 12.5 and 200 kGy, both with magnification 200x (Figure 14d). In the morphological analysis carried out by SEM on the fragile fracture of the samples, it can be said that the radiation interfered with the inorganic components present in the PPrec, which decreased.

3.1.5. Shore D analysis

Figure 15 shows the results obtained for the surface hardness - Shore D, according to ASTM D2240[36], of the PPrec samples with irradiation doses of 12.5, and 25 kGy. The results showed that there were no changes in the surface hardness of the samples at the irradiation doses studied, obtaining an average value of 65.

3.2. Mechanical analysis

3.2.1. Tensile strength at break

Figure 16 shows the results obtained for the tensile strength at break (MPa) of the non-irradiated PPrec samples and those irradiated with doses of 12.5 and 25 kGy. In the irradiated samples, there was a small decrease in the stress at the breaking point due to the radiation. The degradation at a higher irradiation dose is under previous observation by Samat et al.[11]. The higher the radiation dose, the lower the stress at the breaking point due to the breaking (scission) of the PP molecular chains compared to the non-irradiated sample[12]. The PPrec exhibits a

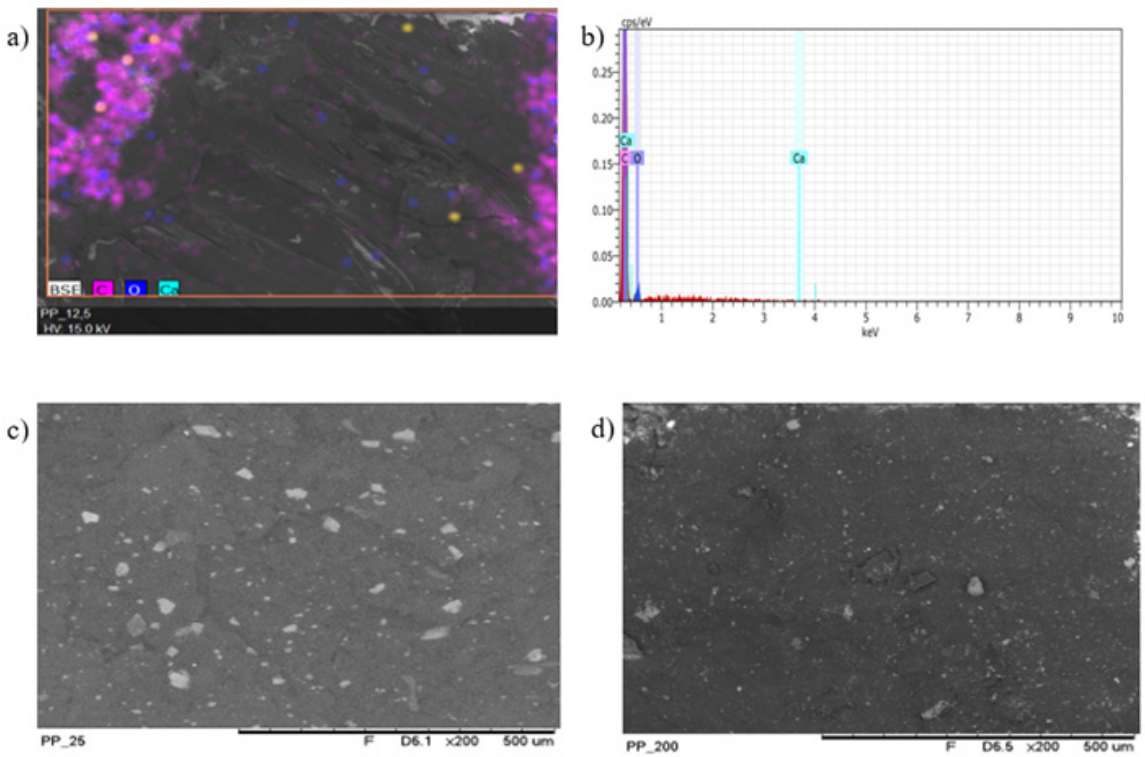

Figure 14. Micrographs of PPrec irradiated with different doses (a, c, d) and EDS (b).

higher degree of crosslinking due to electron beam irradiation, which also enhances the modulus and stiffness of the material[11]. In another study[9], the effects of γ-radiation reduced the molar mass of PPrec, resulting in a decrease in elongation at break.

3.2.2. Tensile strength at yield

Figure 17 shows the tensile strength at yield (MPa) results of the non-irradiated PPrec samples and those irradiated with doses of 12.5 and 25 kGy. In the irradiated samples, there was a decrease in the stress at the yield point due to the radiation[9]. The higher the irradiation dose, the lower the stress at the yield point due to the breaking (splitting) of the PPrec molecular chains compared to the non-irradiated sample. Zerhusen et al.[9] observed that the change to the sample after reprocessing in cycle 2 was not significant; moreover, the elongation at break of the irradiated sample from cycle 3 decreased significantly. The deformation (elongation) decreased dramatically in the irradiated samples compared to the non-irradiated sample. The modulus of elasticity, which is the stress/strain ratio, increased, i.e., the irradiated materials became stiffer due to the radiation. These stress-strain tests also showed a reduction in deformation (elongation)[12], which is not shown in this study.

3.2.3. Izod impact analysis

Figure 18 shows the results of the Izod impact resistance of the non-irradiated and irradiated PPrec samples at doses of 12.5 and 25 kGy. In the irradiated samples, there was a significant decrease in impact resistance due to radiation[1]. The higher the irradiation dose, the lower the impact resistance due to the breaking (splitting) of the PPrec molecular chains compared to the non-irradiated sample. The tensile strength increased with the irradiation dose up to a dose of 30 kGy, as studied by researchers[1]. Moreover, changes in the modulus values were noted along with the increase in the irradiation dose level beyond 50 kGy[11]. Krämer et al.[1] investigated converting a polymer like PP from an injection molding grade (high MFR) to an extrusion grade (low MFR), and observed that the shear thinning is beneficial as it enhances resistance to sagging when the extrudate exits the die; and a result of melt-mixing, an initial material degradation was indicated by a slight decrease in modulus and strength.

3.2.4. Charpy impact analysis

Figure 19 shows the Charpy impact resistance results of the non-irradiated and irradiated PPrec samples at doses of 12.5 and 25 kGy. In the irradiated samples, there was a significant decrease in Charpy impact resistance due to the radiation. The

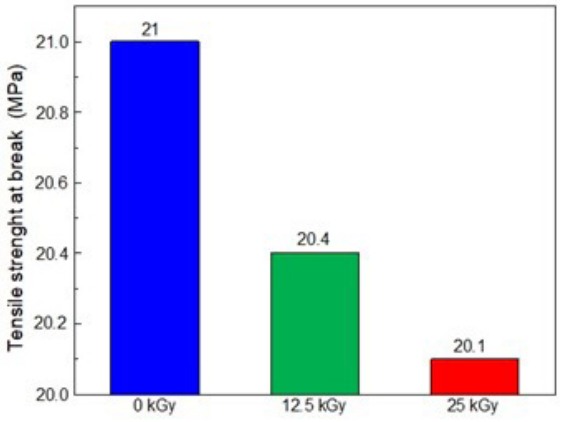

Figure 16. Tensile strength at break of non-irradiated PPrec samples and irradiated with doses of 12.5 and 25 kGy.

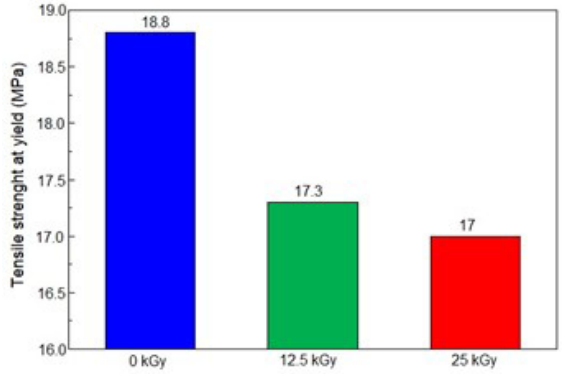

Figure 17. Tensile strength at yield of non-irradiated PPrec samples and irradiated with doses of 12.5 and 25 kGy.

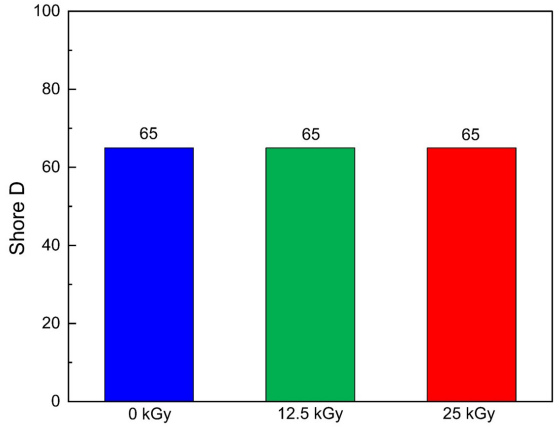

Figure 15. Shore D results of non-irradiated PPrec samples and irradiated with doses of 12.5, and 25 kGy.

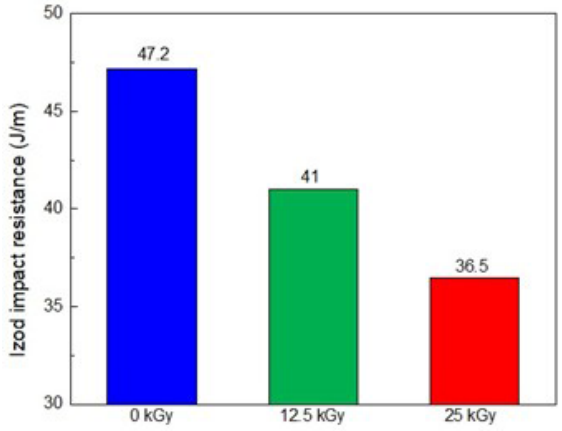

Figure 18. Izod impact resistance of non-irradiated PPrec samples and irradiated with doses of 12.5 and 25 kGy.

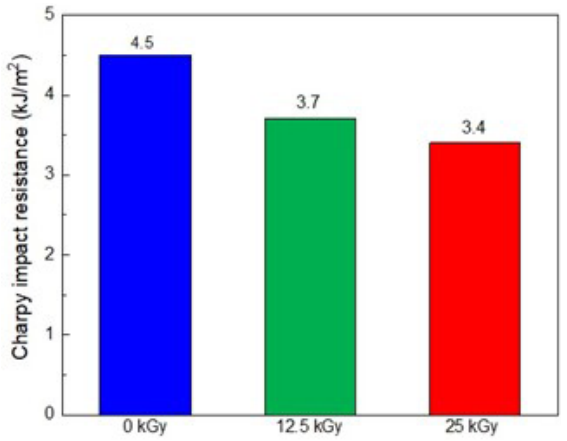

Figure 19. Charpy impact resistance of non-irradiated PPrec samples and irradiated with doses of 12.5 and 25 kGy.

higher the irradiation dose, the lower the impact resistance due to the scission of the lengths of the PPrec molecular chains. The impact strength of crystalline polymers is closely related to their modulus of elasticity, and stress/strain, i.e., the samples of irradiated materials became stiffer and more fragile with radiation[10]. Abiona and Osinkolu[12], observed that the melting temperature and crystallinity reduce as irradiation doses increase, reduction in elongation to fracture and tensile strength of the materials as dose increases. Dahal et al.[6] studied a similar effect of the PP/LLDPE blend, where irradiation can also initiate degradation/scission due to the formation of weak points, defects in the structure, and lower crystallinity.

3.3. Toxicology

Development of vegetable seedlings grown in non-irradiated and irradiated PPrec trays with doses of 12.5 and 25 kGy (Figure 20). After planting, they were monitored

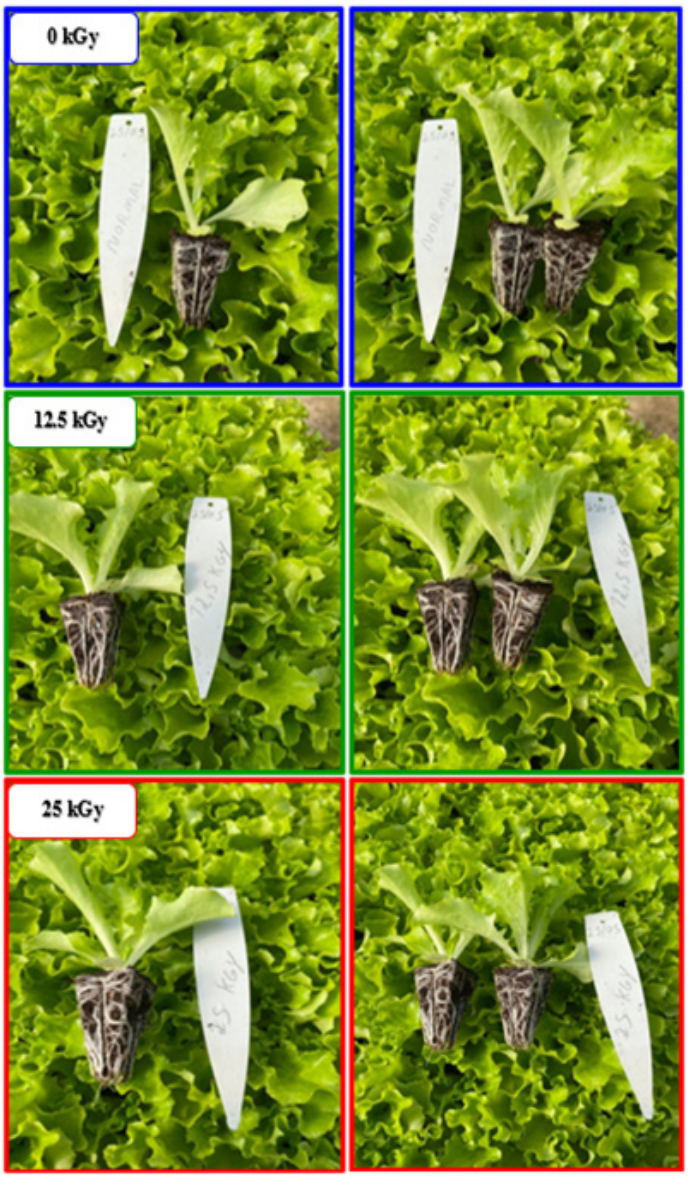

Figure 20. Images of lettuce seedlings grown in non-irradiated PPrec trays and irradiated with doses of 12.5 and 25 kGy.

with fertigation with macro- and micronutrients to check for possible influences on their foliar (leaf) and radicular (root) development. The results were assessed in June 2023, 32 days after planting and roots washed, as shown in Figures 21a and 21b. The images of lettuce seedlings removed from the trays to observe the growth roots (Figure 21b) in non-irradiated PPrec trays and irradiated with doses of 12.5 and 25 kGy, in which checks were made for possible influences on their environmental development nature, also left the roots and washed, for observe the possible influences of radiation on their development, formation, and lettuce growth. During irradiation, radicals are generated, which may react with antioxidants, leading to the formation of radiolysis products and a reduction in antioxidant concentration in fresh lettuce[37].

Table 1 shows the lettuce properties measured after irradiation processing.

Arkatkar et al.[32] studied *in vitro* biodegradation of unpretreated and thermally pretreated polypropylene films by mixed soil culture from a local plastic dumping site. The methyl group index decreased in both cases, indicating that oxidation at the primary carbon was identified by FTIR, after 12 months without changes in the mixed culture. Thus, in the results obtained, the sample analyses show changes in the growth induced by 12.5 and 25 kGy irradiation doses.

3.3.1. Particle size analysis

Figure 22 shows the results obtained for the particle size of the PPrec samples that were not irradiated and were irradiated with doses of 150, 200, 250, 300, 350, 430, and 480 kGy. The use of ball mills proved not to be a technologically efficient method, as the yields found were much lower than expected (below 2.0%) for an ideal particle size (diameter ≤ 1 mm), and a very long exposure time (> 6 hours) was required for all the samples. On the other hand, the knife mills were not ideal either, due to the problem of material agglutination on the rotating cutting knives. The ideal would be to use mills for micronizing plastics (large volumes), which are operated with rotating discs and cooled with liquid nitrogen. The particle size method is used to improve and evaluate the surface area of the PPrec and facilitate production of the masterbatches incorporated with PP neat.

3.3.2. GPC analysis

Figure 23 shows the results obtained for the molar mass of the non-irradiated and irradiated PP samples with doses of 12.5, 25, and 50 kGy.

Table 2 shows the results obtained for the molar mass of the non-irradiated and irradiated PP samples with doses of 12.5, 25, and 50.0 kGy.

Up to 50 kGy, the molar mass (Mn, Mw) decreases in the samples due to the partial breaking of chemical bonds and cross-linking of PP chains. The Mz ratio does not significantly change after the irradiation process, as measured by GPC. The samples irradiated with doses above 100 kGy and up to 500 kGy could not be analyzed because the samples were cross-linked, making it impossible to dissolve them in the solvent used, trichlorobenzene (TCB). The reduction in molar mass is directly linked to rheological properties, and a decline in zero viscosity with increasing irradiation dose and duration has been previously reported in the literature[9,38]. Liu et al.[38]

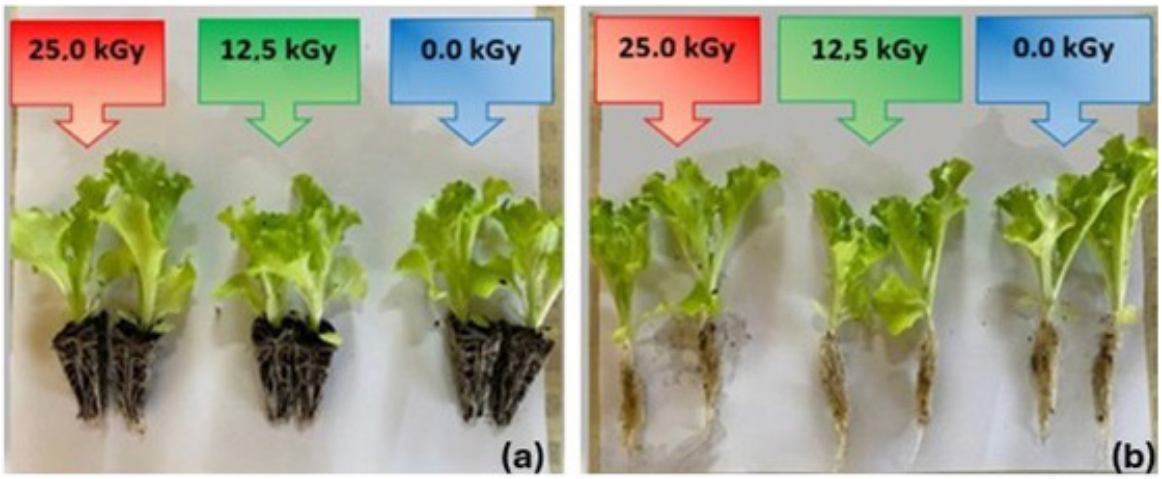

Figure 21. Images of lettuce seedlings taken (a) and washed (b) from trays of non-irradiated PPrec trays and irradiated with doses of 12.5 kGy and 25 kGy.

Table 1. Lettuce properties after irradiation processing with doses of 0, 12.5, and 25 kGy. The different letters represent significant differences in the statistical analysis ($p < 0.05$; ANOVA followed by Tukey's test).

	Control	0 kGy	12.5 kGy	25 kGy
Lettuce germination (%)	100	95	94	95
Leaf weight (g)	3.0 ± 0.2^{a}	3.2 ± 0.4^{b}	3.4 ± 0.3^{c}	3.3 ± 0.4^{b}
Fresh mass (g)	12.5 ± 0.3^{b}	12.3 ± 0.2^{b}	12.8 ± 0.6^{c}	11.9 ± 0.4^{a}
Dry mass (%)	0.95	0.91	0.93	0.90
Mass variation (%)	0.01	0.01	0.02	0.01

Table 2. The molar mass of PP samples was non-irradiated and irradiated with doses of 12.5, 25, and 50 kGy.

Molar mass (Dalton)	0 kGy	12.5 kGy	25 kGy	50 kGy
Mn	63632	52626	63215	40710
Mw	544435	437149	414672	385314
Mz	2279000	1938000	1938000	2230000
Mw/Mn	9	8	7	9

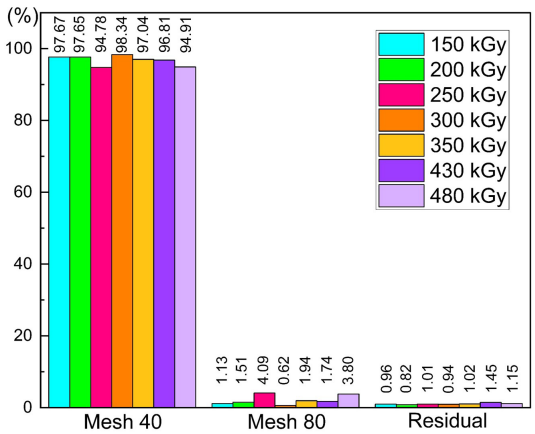

Figure 22. Granulometry results of non-irradiated PPrec samples and irradiated with doses of 150, 200, 250, 300, 350, 430, and 480 kGy.

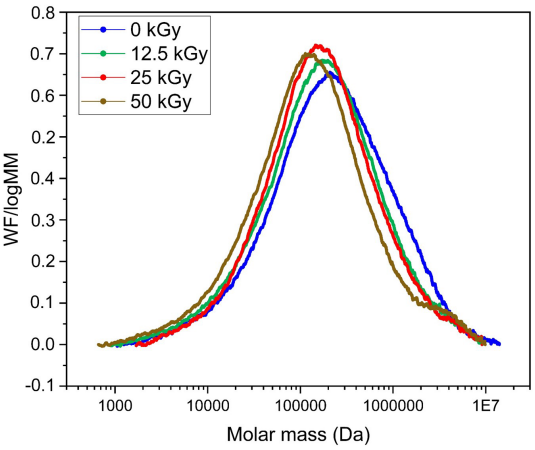

Figure 23. The molar mass of non-irradiated PP samples and irradiated with doses of 12.5, 25.0, and 50 kGy.

evaluated the effects of Cobalt-60 gamma source from 250 to 1000 kGy dose, the Mw of iPP remains largely unchanged, with only an increase observed in the low Mw fraction of the distribution, due to the gamma ray irradiation induces substantial chain scission in iPP, detected by GPC analysis.

4. Conclusions

The results found were quite enlightening and compare the analysis of the results of PPrec using ionizing radiation. The results of the mechanical, physical, and morphological properties found from ionizing radiation allowed us to carry out broader studies into the applications of recycled polypropylene in other types of plastic parts for a critical analysis of recyclability, cost, and the environment.

Ionizing radiation up to a dose of 25 kGy can be considered beneficial for the reuse of PP for recycling and reuse of the parts produced, as long as they are not subjected to thermally, chemically, and mechanically aggressive environments and cost and performance analyses are carried out. The applications of ionizing radiation were very important in the field of polymers, where very few people know about the irradiation process. There are many gaps in studies on the subject that need to be filled with the evolution of new technologies and applications of radiation. Ionizing radiation up to a dose of 25 kGy was considered beneficial for the reuse of polypropylene for recycling and reuse of the parts produced, provided that they are not subjected to thermally, chemically, or mechanically aggressive environments. Subsequently, cost and performance analyses should be carried out.

The results of the mechanical properties of traction, elongation, and impact up to an irradiation dose of 25 kGy were considered admissible for similar applications in a static regime. Above this dose of 25 kGy, these mechanical properties were compromised and are not recommended where parts are needed for these requirements. The greatest difficulty was when the parts are produced by injection molding, blow molding, and thermoforming. The melting temperature decreased when irradiated with a dose of up to 250 kGy, and increased when irradiated with a dose of 250 to 500 kGy due to molecular cross-linking of the PPrec.

Up to this dose of 50 kGy, the advantage of applying radiation to control molecular shear to obtain shorter molecular chain lengths in PP rec, which could be used as a carrier for additives in paints, adhesives, and plastics, and/or as a flow modifier for injection molding of large and/or thin-walled parts. Above the 50 kGy dose, the formation of cross-links began (cross-linked PP), which could be used as fillers for asphalt, construction, and other applications. Profound changes were observed in the morphology of polypropylene when subjected to the gamma-ray irradiation process. The lettuce samples submitted to the toxicity test did not show any significant changes after irradiation processing, thus maintaining their characteristics for agricultural application. The physical, mechanical, thermal, and chemical properties must be analyzed in each case of application for the PP products manufactured. Applying an irradiation dose of up to 12.5 kGy or even less was enough to be able to reuse the trays and other types of plastic products, injected or not (blown bottles, thermoformed parts, containers) made from recycled polypropylene, so that they could be reused and not discarded.

5. Acknowledgments

The authors thank Comissão Nacional de Energia Nuclear (CNEN) and Coordenação de Aperfeiçoamento de Pessoal de Nível Superior (CAPES) for grants, Henkel® and

Thermoblend® for the analyses, and the electron accelerator facility at the CETER/IPEN.

6. References

1. Krämer J, Guedes de la Cruz GC, Kern W, Roitner J, Witschnigg A, Rittmannsberger F, et al. Increasing the melt viscosity of post-consumer recycled polypropylene via E-Beam techniques. Radiat Phys Chem. 2024;222:111846. http://doi.org/10.1016/j.radphyschem.2024.111846.
2. Maksoud M, Kassem S, Ashour A, Awed A. Recycled high-density polyethylene plastic reinforced with ilmenite as a sustainable radiation shielding material. RSC Advances. 2023;13(30):20698-708. http://doi.org/10.1039/D3RA03757F.
3. Dobránsky J, Pollák M, Behálek L, Svetlík J. Implementation of a recycled polypropylene homopolymer material for use in additive manufacturing. Sustainability. 2021;13(9):4990. http://doi.org/10.3390/su13094990.
4. U.S. Environmental Protection Agency. 2019 year in review [Internet]. Washington, DC: EPA; 2019 [cited 2025 Jan]. Available from: https://www.epa.gov/sites/default/files/2020-02/documents/hq_2019_year_in_review.pdf
5. Almeida L, Cota A, Rodrigues D. Saneamento, arboviroses e determinantes ambientais: impactos na saúde urbana. Cien Saude Colet. 2020;25(10):3857-68. http://doi.org/10.1590/1413-812320202510.30712018.
6. Dahal P, Kim J, Kim Y. Effects of linear low density polyethylene on physical properties and irradiation effectiveness of polypropylene. Korean J Chem Eng. 2014;31(1):1-5. http://doi.org/10.1007/s11814-013-0189-2.
7. Jiang Q, Wu Y, Lu X, Wu J, Liu L, Gao Y, et al. Stepwise crystallization method combining isotactic polypropylene-based plastic waste film to prepare high-performance polypropylene random copolymer. Polymer. 2024;308:127372. http://doi.org/10.1016/j.polymer.2024.127372.
8. Zhiltsova T, Oliveira M. Sustainable polypropylene blends: balancing recycled content with processability and performance. Polymers. 2025;17(11):1556. http://doi.org/10.3390/polym17111556.
9. Zerhusen N, Herrmann S, Susoff M, Petersen S. Stability assessment of a commercial polypropylene copolymer and Irgafos 168 under repeated injection molding and γ-irradiation cycles. J Appl Polym Sci. 2024;141(10):e55071. http://doi.org/10.1002/app.55071.
10. Żenkiewicz M, Kurcok M. Effects of compatibilizers and electron radiation on thermomechanical properties of composites consisting of five recycled polymers. Polym Test. 2008;27(4):420-7. http://doi.org/10.1016/j.polymertesting.2008.01.002.
11. Samat N, Motsidi S, Lazim N. Effects of electron beam radiation dose on the compatibilization behaviour in recycled polypropylene/microcrystalline cellulose composites. IOP Conf Series Mater Sci Eng. 2018;290:012034. http://doi.org/10.1088/1757-899X/290/1/012034.
12. Abiona A, Osinkolu A. Gamma-irradiation induced property modification of polypropylene. Int J Phys Sci. 2010;5(7):960-7.
13. Uzun I. Methods of determining the degree of crystallinity of polymers with X-ray diffraction: a review. J Polym Res. 2023;30(10):394. http://doi.org/10.1007/s10965-023-03744-0.
14. Chukhchin D, Malkov A, Tyshkunova I, Mayer L, Novozhilov E. Diffractometric method for determining the degree of crystallinity of materials. Crystallogr Rep. 2016;61(3):371-5. http://doi.org/10.1134/S1063774516030081.
15. ASTM: American Society for Testing and Materials. ASTM D638: standard test method for tensile properties of plastics. West Conshohocken: ASTM; 2022.
16. ASTM: American Society for Testing and Materials. ASTM D256: standard test methods for determining the izod pendulum impact resistance of plastics. West Conshohocken: ASTM; 2024.
17. ASTM: American Society for Testing and Materials. ASTM D6110: standard test method for determining the charpy impact resistance of notched specimens of plastics. West Conshohocken: ASTM; 2018.
18. ASTM: American Society for Testing and Materials. ASTM D785: standard test method for rockwell hardness of plastics and electrical insulating materials. West Conshohocken: ASTM; 2015.
19. ASTM: American Society for Testing and Materials. ASTM D1921: standard test methods for particle size (sieve analysis) of plastic materials. West Conshohocken: ASTM; 2018.
20. ABNT: Associação Brasileira de Normas Técnicas. NBR7181: solo — análise granulométrica. Rio de Janeiro: ABNT; 2025.
21. Samat N, Yahya M, Lazim N. The compatibility effects of irradiated recycled PP on the mechanical and water properties of recycled PP/microcrystalline cellulose composites. AIP Conf Proc. 2016;1774(1):020008. http://doi.org/10.1063/1.4965056.
22. Kida T, Hiejima Y, Nitta K. Molecular orientation behavior of isotactic polypropylene under uniaxial stretching by rheo-Raman spectroscopy. Express Polym Lett. 2016;10(8):701-9. http://doi.org/10.3144/expresspolymlett.2016.63.
23. Gopanna A, Mandapati R, Thomas S, Rajan K, Chavali M. Fourier transform infrared spectroscopy (FTIR), Raman spectroscopy and wide-angle X-ray scattering (WAXS) of polypropylene (PP)/cyclic olefin copolymer (COC) blends for qualitative and quantitative analysis. Polym Bull. 2019;76(8):4259-74. http://doi.org/10.1007/s00289-018-2599-0.
24. Nielsen A, Batchelder D, Pyrz R. Estimation of crystallinity of isotactic polypropylene using Raman spectroscopy. Polymer. 2002;43(9):2671-6. http://doi.org/10.1016/S0032-3861(02)00053-8.
25. Furukawa T, Sato H, Kita Y, Matsukawa K, Yamaguchi H, Ochiai S, et al. Molecular structure, crystallinity and morphology of polyethylene/polypropylene blends studied by Raman mapping, scanning electron microscopy, wide angle X-ray diffraction, and differential scanning calorimetry. Polym J. 2006;38(11):1127-36. http://doi.org/10.1295/polymj.PJ2006056.
26. Chalmers J, Edwards H, Lees J, Long D, Mackenzie M, Willis H. Raman-spectra of polymorphs of isotactic polypropylene. J Raman Spectrosc. 1991;22(11):613-8. http://doi.org/10.1002/jrs.1250221104.
27. Prokhorov KA, Nikolaeva GY, Sagitova EA, Pashinin PP, Guseva MA, Shklyaruk BF, et al. Raman structural study of melt-mixed blends of isotactic polypropylene with polyethylene of various densities. Laser Phys. 2018;28(4):045702. http://doi.org/10.1088/1555-6611/aaa9f7.
28. Pinheiro G, Dipold J, Freitas A, Vasconcelos K, Wetter N. The effect of gamma-irradiated recycled polyolefins as asphalt binder modifiers. Road Mater Pavement Des. 2025;26(sup1):417-42. http://doi.org/10.1080/14680629.2025.2489028.
29. Báez M, Hendra P, Judkins M. The Raman spectra of oriented isotactic polypropylene. Spectrochim Acta A Mol Biomol Spectrosc. 1995;51(12):2117-24. http://doi.org/10.1016/0584-8539(95)01512-1.
30. Oliani W, Komatsu L, Lugao A, Parra D. Thermal ageing and accelerated weathering of HMSPP: structural and morphological studies. Macromol Symp. 2016;367(1):18-23. http://doi.org/10.1002/masy.201500135.
31. Oka T, Oshima A, Motohashi R, Seto N, Watanabe Y, Kobayashi R, et al. Changes to the chemical structure of isotactic-polypropylene induced by ion-beam irradiation. Radiat Phys Chem. 2011;80(2):278-80. http://doi.org/10.1016/j.radphyschem.2010.07.047.
32. Arkatkar A, Arutchelvi J, Bhaduri S, Uppara P, Doble M. Degradation of unpretreated and thermally pretreated polypropylene by soil consortia. Int Biodeterior Biodegradation. 2009;63(1):106-11. http://doi.org/10.1016/j.ibiod.2008.06.005.
33. Rivaton A, Lalande D, Gardette J. Influence of the structure on the γ-irradiation of polypropylene and on the post-irradiation effects. Nucl Instrum Methods Phys Res B. 2004;222(1-2):187-200. http://doi.org/10.1016/j.nimb.2004.02.012.
34. Allayarov SR, Confer MP, Rudneva T, Demidov SV, Nikolskii VG, Chekalina SD, et al. Influence of γ-radiation input dose and

post-radiation high temperature shear grinding on polypropylene functional group composition. Polym Degrad Stabil. 2024;220:110631. http://doi.org/10.1016/j.polymdegradstab.2023.110631.
35. Al-Ghamdi H, Farah K, Almuqrin A, Hosni F. FTIR study of gamma and electron irradiated high-density polyethylene for high dose measurements. Nucl Eng Technol. 2022;54(1):255-61. http://doi.org/10.1016/j.net.2021.07.023.
36. ASTM: American Society for Testing and Materials. ASTM D2240: standard test method for rubber property—durometer hardness. West Conshohocken: ASTM; 2021.
37. Celiz M, Morehouse K, de Jager L, Begley T. Concentration changes of polymer additives and radiolysis products in polyethylene resins irradiated at doses applicable to fresh produce. Radiat Phys Chem. 2020;166:108520. http://doi.org/10.1016/j.radphyschem.2019.108520.
38. Liu B, Gao Y, Li J, Guo C, Gao J, Chen Y, et al. Aging behavior of polypropylene as cable insulation under gamma-ray irradiation. IEEE Trans Dielectr Electr Insul. 2024;31(2):956-64. http://doi.org/10.1109/TDEI.2023.3337753.

Data Availability

The entire dataset supporting the results of this study was published in the article itself.